Vol 4 (1) (2023)

Measurement, Control, and Automation

Website: https:// mca-journal.org

ISSN 1859-0551

A novel load - frequency control scheme applying fuzzy logic technique for two-area interconnected power systems with renewable energy sources

Diem-Vuong Doan[1], Ngoc-Khoat Nguyen[2*], Quang-Vinh Thai[3]

[1] *Faculty of Control and Automation, Electric Power University*
[2] *Institute of Information Technology, Vietnam Academy of Science and Technology*
[*]*Corresponding author E-mail: khoatnn@epu.edu.vn*

Abstract

This paper proposes a novel intelligent control algorithm in dealing with the load-frequency control problem of a two-area interconnected thermal power system. This control methodology applying a modified PID controller with three parameters tuned by a reasonable fuzzy logic inference structure. The control plant of this study is a two - area interconnected electric thermal power grid model using reheat and non-reheat turbines together with renewable energy sources such as wind power and solar energy. This model is mathematically established at first and the load-frequency control solution employing the proposed fuzzy logic-based PID controllers is implemented successfully in MATLAB/Simulink environment. The numerical simulation results obtained in various scenarios compared with those of the conventional regulators and a number of existed intelligent load-frequency counterparts demonstrate the high effectiveness and applicability of the proposed control strategy.

Keywords*: Load Frequency Control (LFC), PID-like fuzzy logic controller, renewable energy sources, nonlinearities.*

Symbols

Symbols	Units	Description
R	Hz/p.u.	Speed regulation of the governor
T_g	s	Time constant of speed governor
T_{ch}	s	Non–reheat time constant
T_{rh}	s	Low pressure reheat time constant
F_{hp}		High pressure stage
T_{wts}	s	Time constant of wind turbine
T_{spv}	s	Time constant of solar power
Δf	Hz	Change in frequency
ΔP_g	p.u.	Change in electrical power
ΔP_c	p.u.	The speed governor senses the difference between reference power
ΔP_t	p.u.	Change in the valve position

Abbreviations

GDB	Governor Dead Band
GRC	Generation Rate Constraint
LFC	Load Frequency Control
ACE	Area Control Error
PSO	Particle Swarm Optimization
GWO	Grey Wolf Optimizer
FPID	Fractional PID
GA	Genetic Algorithm

Tóm tắt

Bài báo này đề xuất một giải thuật điều khiển thông minh mới để giải quyết bài toán điều khiển tần số - phụ tải của một hệ thống nhiệt điện hai vùng kết nối. Thuật toán đề xuất ứng dụng một bộ điều chỉnh PID cải tiến với ba tham số được chỉnh định bởi một cấu trúc logic mờ thích hợp. Đối tượng điều khiển của nghiên cứu này là một mô hình hệ thống nhiệt điện hai vùng kết nối sử dụng các tuabin hồi nhiệt và không hồi nhiệt cùng với các nguồn năng lượng tái tạo như năng lượng gió và năng lượng mặt trời. Hệ thống điện này được mô hình hóa trước tiên và giải pháp điều khiển tần số - phụ tải sử dụng bộ điều khiển PID cải tiến dựa trên logic mờ sẽ được thực hiện thông qua phần mềm MATLAB/Simulink. Các kết quả mô phỏng số thu được trong nhiều trường hợp giả định khác nhau được so sánh với các bộ điều chỉnh truyền thống và một số các bộ điều khiển tần số-phụ tải thông minh trước đó đã chứng minh sự hiệu quả và khả năng ứng dụng cao của chiến lược điều khiển đã đề xuất.

1. Introduction

Load-frequency control (LFC) is one of the most crucial control strategies to ensure the stability and economy of an interconnected power system [1–3]. In [4], the LFC of three areas is unequal bonding heat, wind and hydrogen. The generating unit has been developed with the Proportional Integral (PI) controller. In paper [5], a new load frequency controller based on Type-2 Fuzzy Quasi-Decentralized Functional Observe (T2FQFO) is recommended. The LFC strategy aims to continuously monitor the system frequency as well as the tie-line power flow.

Received: 14 February 2023; Accepted: 17 March 2023

According to the constrained current deviation control theory, the LFC scheme calculates the net change of two such parameters relative to their nominal value, known as the area control error (ACE), to control valve setting of the main engine with the goal of forcing the ACE signals to meet acceptable values. The LFC strategy directs the ACE signal to the desired values, which means that both the frequency offset and the tie-line power are considered to be close to zero within the allowed tolerances. It can be found that a huge number of studies have been conducted for the LFC issue. Obviously, many control and optimization techniques such as conventional ones [6], optimal control [7], genetic algorithm (GA) [8], particle swarm optimization (PSO) [9], bacteria foraging optimization algorithm (BFOA) [10] have also been used in dealing with the LFC problem. A smart grid is becoming an important goal in the current and future power system network configuration [11]. The new modern grids provide real-time networks, rapid fault analysis and also dedicate the ability to connect a large number of renewable energy sources into the power system [12]. The rapid development of global industry and business has caused a significant shortage of available energy in case of excessive use of fossil fuels [13]. As well as concerns about safe sources, environmental concerns invested in low-carbon power generation technology is one of the priorities following an energy program in many countries around the world [14,15].

Therefore, generating electricity from renewable energy sources is a viable option that will not only meet the growing energy demand but also take care of the environment [16]. The integration of RE sources poses additional uncertainties and challenges to the power system, since RES is discontinuous and. Their locations are geographically dispersed [17]. The penetration of different renewable energy sources in modern interconnected electrical systems can significantly reduce the inertia of the system. When converting renewable energy sources to power interconnected power system using converters/inverters, such power electronic interfaces will reduce the total inertia of the system and reduce voltage stability/ frequency compared to conventional synchronous generator sets.

Therefore, reducing enough inertia will be one of the main limitations of grid-connected renewable energy sources in the world. By increasing the penetration of existing renewable energy sources, the inertia of the connected electrical system may be insufficient, creating dynamic problems for the system's stable voltage and frequency and cause negative effects on the stability/resiliency of the power system [18,19]. In [20], if the large wind generation is stalled due to a fault, it can harm the operation of the power system and lead to load frequency control problems. The primary target of LFC is on maintaining the constant frequency over the arbitrarily changing active power loads that as well termed as unidentified explicit disturbance. An additional target of LFC is on regulating the tie-line power exchange error [21-24]. The interconnected power system when adding renewable energy sources is a practical need in modern life.

However, it reduces the inertia of the system and increases the frequency oscillations of the areas, and at the same time increases the frequency of the system together with power dynamics on power transmission lines.

These include devices with nonlinear system components such as GDB, GRC, changing operating load conditions and renewable energy sources. The interconnected power system is a complex object, so controlling the system frequency and power on the line encounters difficulties. The above studies have used different methods to stabilize the system frequency, but they do not consider the system in many cases such as the existence of nonlinear factors, the continuous system parameters changing and the addtion of renewable energy sources. To solve the LFC problems, not only the traditional PID controllers have been widely used but also intelligent counter parts, i.e. fuzzy logic - based controllers (FLC) have attracted researchers and engineers. Applying these FLCs, it is clear control systems with a lot of unknown parameters as well as uncertainties can be completely conducted with promising criteria. One of the most popular and efficient FLCs used, especially for the LFC, is PID-like FLC. This study proposes a fully feasible LFC scheme applying the PID-like FLC for a complex two - area interconnected power system with nonlinearities i.e. GRC and GDB as well as renewable energy sources. The superiority of the proposed approach is shown by comparing the results with a number of conventional controllers in dealing with the LFC problem. The rest of this paper is organized as follows. Section 2 presents the modelling of an interconnected power system focusing on the LFC problem. Then, Section 3 proposes the design of a PID-like FLC methodology, which will be applied for the LFC. Next, Section 4 provides simulation results implemented in MATLAB/Simulink environment to verify the effectiveness of the proposed control strategy. At last, conclusions and discussions regarding this study will also be given in Section 5.

2. Modelling of interconnected power systems in load frequency control

The first step to study a control system is to establish the mathematical of the control plant. It is the fact that mathematical modelling of an isolated power system is constituted of the following elements:

(i) Speed governor model
(ii) Thermal turbine model
(iii) Wind turbine and solar power model
(iv) Generator load model
(v) Tie- lines

2.1. Speed governor model

Speed governor is a unit used in electrical power systems to sense frequency deviation caused by the load change and cancel it by changing the turbine input. The schematic diagram of a speed governing unit is shown in Figure 1. Where R is the speed regulation of the governor, Tg is time constant of speed governor, Δf is change in frequency, ΔPg is change in electrical power and ΔPc is the speed governor senses the difference between reference power. Without load reference, when the load change occurs, part of the change will be compensated by the valve/gate adjustment while the rest of the change is represented in the form of frequency deviation. The reduced form of Figure 1 is shown in Figure 2.

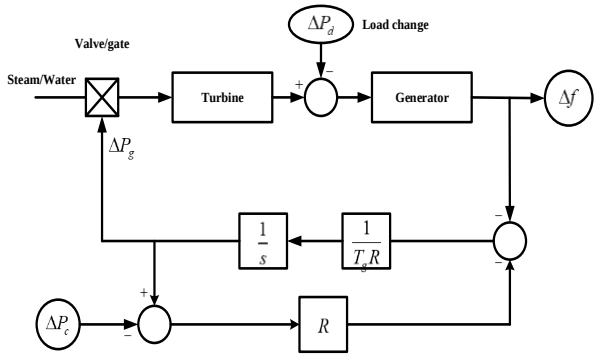

Figure 1: Speed governor unit

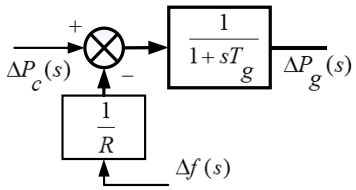

Figure 2: Block diagram of speed governor

The Equation (1) defines a relationship regarding a typical speed governor of an electric power grid:

$$\Delta P_g(s) = \frac{1}{1+sT_g}(\Delta P_C(s) - \frac{1}{R}\Delta F(s)) \quad (1)$$

2.2. Thermal turbine models

A turbine unit in power systems is used to transform the primary energy, such as the energy from steam or water, into mechanical power (ΔP_t) which is supplied to the generator. There are three kinds of commonly used turbines: non-reheat, reheat and hydraulic turbines. All of which can be modelled by transfer functions. The transfer function of the non-reheat turbine is represented as:

$$G_t(s) = \frac{P_t(s)}{P_g(s)} = \frac{1}{1+sT_{ch}} \quad (2)$$

Where *Tch* is non –reheat time constant and ΔP_t is change in the valve position.

Reheat turbines are modelled as second-order units, since they have different stages due to high and low steam pressures. The transfer function can be represented in (3).

$$G_t(s) = \frac{P_t(s)}{P_g(s)} = \frac{F_{hp}T_{rh}s+1}{T_{rh}s+1} \cdot \frac{1}{T_{ch}s+1} \quad (3)$$

Where *Trh* and *Fhp* are low pressure reheat time constant and high pressure stage, respectively.

2.3. Wind turbine and solar power model

2.3.1. *Wind turbine model*

The wind turbine consists of a turbine-generator shaft mechanism, which is used to convert the rotor rotation into electrical energy. The following equation (4) represents the mechanical output of the wind turbine and is defined as follows:

$$P_{WT} = \frac{1}{2}\rho A C_p(\lambda,\beta)V_W^3 \quad (4)$$

Where λ, ρ, Vw, Cp are speed ratio, air density factor (Kg/cu.m), wind speed (m/s) and power coefficient, respectively.

$$\Delta P_{wt} = \begin{cases} 0, & V_w < V_{cut-in} \\ 0, & V_w > V_{cut-out} \\ 0, & V_{rated} \le V_w \le\le V_{cut-out} \\ [0.007872V_w^5 & else \\ -0.23015V_w^4 & \\ +1.3256V_w^3 + 11.061V_w^2 & \\ -102.2V_w + 2.33]\Delta V_w & \end{cases} \quad (5)$$

For small signal stability of the system, the rate of change of wind power output given in (6) has been considered for assessing the stability of the proposed systems. The first-order transfer function model of wind turbine is shown as:

$$\frac{\Delta P_{wtg}(s)}{\Delta P_{wt}(s)} = \frac{1}{T_{wts}s+1} \quad (6)$$

Where T_{wts} is the time constant of wind turbine.

2.3.2. *Solar power model*

The transfer function model of a solar power is given in (7).

$$\frac{\Delta P_{spv}(s)}{\Delta P_{sp}(s)} = \frac{1}{T_{spv}s+1} \quad (7)$$

Where T_{spv} is time constant of solar power

2.4. Generator load model

A generator unit in electrical systems converts mechanical energy received from a turbine into electrical energy. But for the interconnected power systems, the focus is on the generator's rotor speed (power system frequency) output rather than energy conversion. Since electrical energy is difficult to store in large quantities, a balance must be maintained between the energy generated and the load demand. When a load change occurs, the mechanical energy sent from the turbine will no longer match the electrical energy generated by the generator. The error between mechanical power (ΔPt) and electrical power is incorporated into the rotor speed deviation (ω_r), which can be converted to frequency offset (Δf) by multiplying by 2π .

The electrical load can be decomposed into a resistive load, which remains constant as the rotor speed changes and the motor load changes with the load speed. If the mechanical power does not change, the motor load will compensate for the load change at a different rotor speed than the specified value which is shown in the Figure 3.

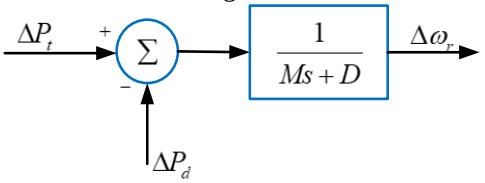

Figure 3: Block diagram of the generator

The mathematical model of generator - load corresponding to Fig. 3 can be obtained below:

$$\Delta \mathrm{F}(s) = \frac{1}{Ms+D}(\Delta P_t(s) - \Delta P_d(s)) \quad (8)$$

Where M is an inertia constant of the generator, D denotes load damping constant and ΔP_d(s) is load demand change

2.5. Tie-lines

In an interconnected power system, different areas are connected to other parts via tie-lines. When the frequencies are in two different areas, an energy exchange occurs through the line connecting the two areas. The tie-line connections can be considered as a mathematical model shown in Figure 4.

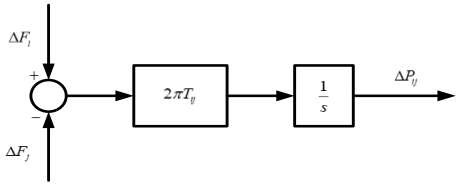

Figure 4: Block diagram of tie-lines

The Laplace transform representation of the block diagram in Figure 4 is given by:

$$\Delta P_{ij} = \frac{2\pi T_{ij}}{s}(\Delta F_i(s) - \Delta F_j(s)) \quad (9)$$

Where ΔP_{ij} is tie-line exchange power between areas i and j, and T_{ij} is the tie-line synchronizing power coefficicnt between areas i and j. From Figure 4, it can be seen that the tie-line power error is the integral of the frequency difference between the two areas.

A block diagram of two-area interconnected power systems with GDB, GRC and renewable energy sources has been shown in Figure 5.

The control objectives of the load-frequency control in multi-area interconnected power system are mainly to control the frequency variation, ACE and tie-line power deviation in the areas towards zero while the system has many nonlinear, uncertain components, time delay and various load conditions.

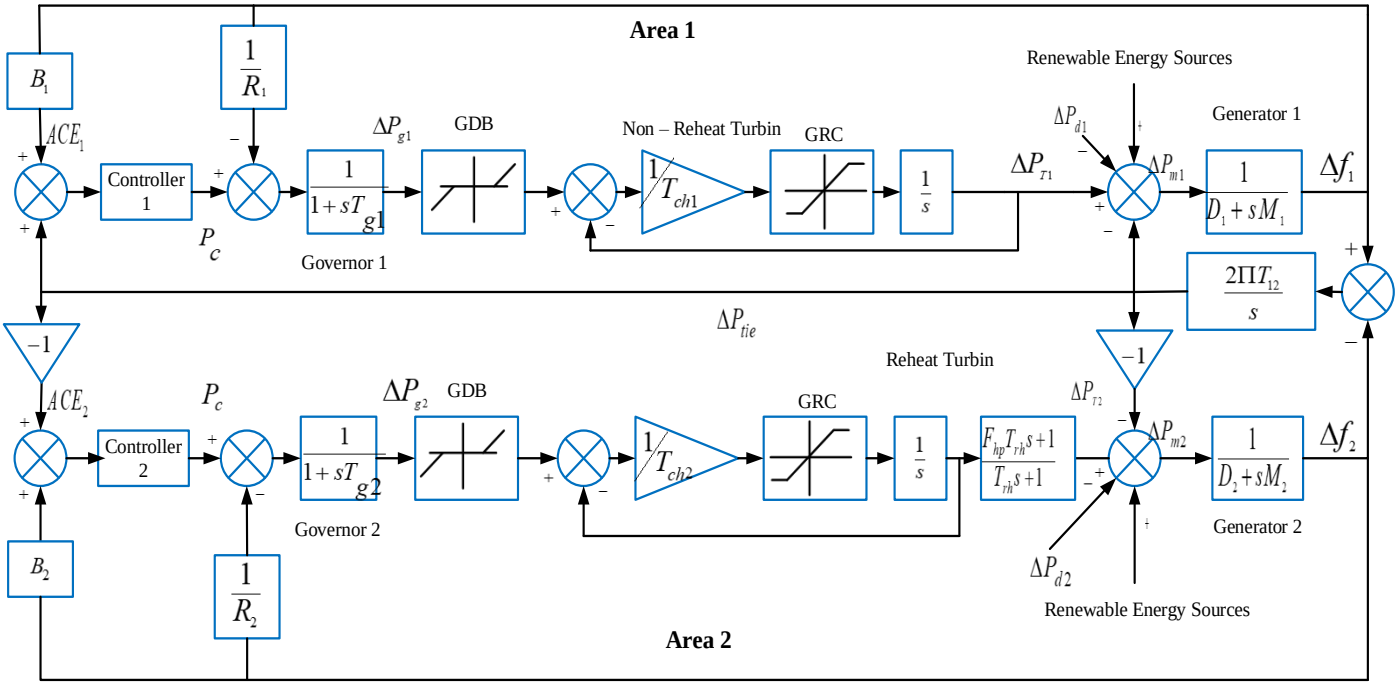

Figure 5: Block diagram of two-area interconnected non-reheat thermal - reheat thermal power system with GRC, GDB and renewable energy sources

3. Design of fuzzy - PID controller

This paper proposes a new PID-based fuzzy logic controller applied for the load - frequency control problem. The working principle of such a PID-fuzzy logic inference structure is depicted in Figure 6. In this context, the PID regulator with three factors *Kp*, *Ki* and and *Kd* are tuned using a reasonable fuzzy logic model.

Fuzzy variables of two inputs ACE and ΔACE are NB, NM, NS, ZO, PS, PM and PB are Negative Big, Negative Medium, Negative Small, Zero, Positive Small, Positive Medium and Positive Big, respectively.

The fuzzy variables of the two inputs *Kp'* and *Kd'* are S, M respectively for Small and Big, respectively.

Fuzzy variables of α are S, MS, MB and B correspond Small, Medium Small, Medium Big and Big.

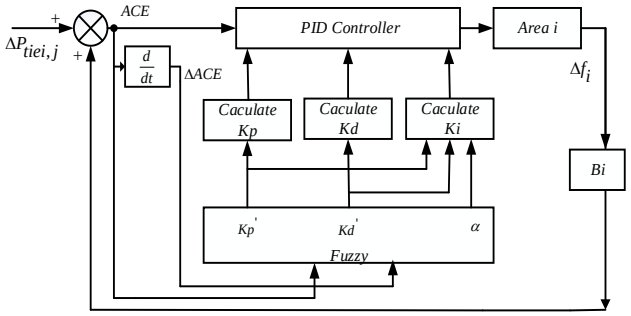

Figure 6: The structure of Fuzzy – PID controller

In Figure 5, three parameters of the PID controller applied for the load frequency control are determined by means of an eficiency. Assuming that two parameters Kp and Kd are always in the ranges [Kp min, Kp max] and [Kd min, Kd max], it is reasonable to define the following equations:

$$K_p' = (K_p - K_{p\min}) / (K_{p\max} - K_{p\min}) \quad (10)$$

$$K_d' = (K_d - K_{d\min}) / (K_{\mathrm{d}\max} - K_{\mathrm{d}\min}) \quad (11)$$

$$T_i = \alpha T_d \quad (12)$$

$$K_i = K_p / \alpha \mathrm{T}_d = {K_p}^2 / (\alpha T_d) \quad (13)$$

$$K_{p\min} = 0.32K_u, \quad K_{p\max} = 0.6K_u \quad (14)$$

$$K_{d\min} = 0.08K_u \mathrm{T}_u, \quad K_{d\max} = 0.15K_u T_u \quad (15)$$

Fuzzy controller designed with inputs ACE and ΔACE has the membership functions presented in Figures 7-9 and Tables 1-3

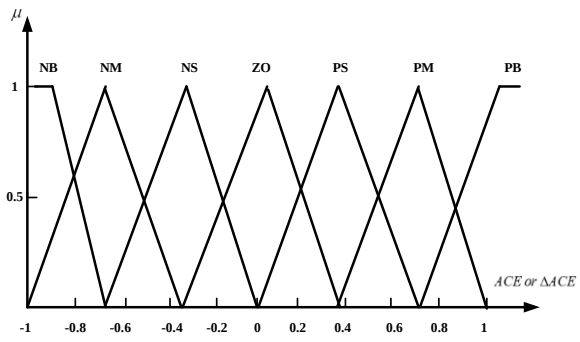

Figure 7: Membership functions of ACE and ΔACE

The outputs of the fuzzy set are Kp', Kd' and α.

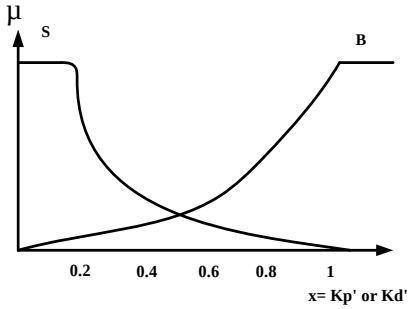

Figure 8: Membership functions of Kp' and Kd'

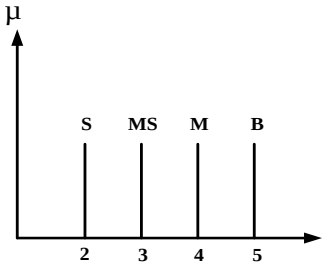

Figure 9: Membership function of α

Table 1: Fuzzy rule for Kp'

ACE	ΔACE						
	NB	NM	NS	ZO	PS	PM	PB
NB	B	B	B	B	B	B	B
NM	S	B	B	B	B	B	S
NS	S	S	B	B	B	S	S
ZO	S	S	S	B	S	S	S
PS	S	S	B	B	B	S	S
PM	S	B	B	B	B	B	S
PB	B	B	B	B	B	B	B

Table 2: Fuzzy rule for Kd'

ACE	ΔACE						
	NB	NM	NS	ZO	PS	PM	PB
NB	S	S	S	S	S	S	S
NM	B	B	S	S	S	B	B
NS	B	B	B	S	B	B	B
ZO	B	B	B	B	B	B	B
PS	S	S	S	S	B	B	B
PM	B	B	S	S	S	B	B
PB	S	S	S	S	B	B	B

Table 3: Fuzzy rule for α

ACE	ΔACE						
	NB	NM	NS	ZO	PS	PM	PB
NB	S	S	S	S	S	S	S
NM	MS	MS	S	S	S	MS	MS
NS	M	MS	MS	S	MS	MS	M
ZO	B	M	S	S	S	M	B
PS	M	MS	MS	S	MS	MS	M
PM	MS	MS	S	S	S	MS	MS
PB	S	S	S	S	S	S	S

From (10), (11) and (13) the following equations can be deduced:

$$K_p = (K_{p\max} - K_{p\min})K_p' + K_{p\min} \quad (16)$$

$$K_d = (K_{\mathrm{d}\max} - K_{d\min})K_d' + K_{d\min} \quad (17)$$

$$K_i = {K_p}^2 / (\alpha T_d) \quad (18)$$

4. Case studies

A numerical simulation process to verify the feasibility of the proposed control strategy plays a significant role in designing an efficient controller. The current study applying MATLAB/Simulink software to implement a number of simulations for this goal. The simulation scenarios described as a system in reality encountered with nonlinearities, variation of different load types, uncertainties and time delay. System

parameters used for simulation in Table 5. The proposed controller is compared with Genetic Algorithm tuned PI (GA PI), Grey Wolf Optimizer tuned PI (GWO PI), Particle Swarm Optimization optimized PI controller (PSO PI), Improved Grey Wolf Optimizer tuned PI (I- GWO PI), PSO GWO PI (fuzzy PI) controller and Fractional PID (FPID) to demonstrate its control quality.

4.1. Performance comparison under different types of load changes including step load disturbance, pulse load deviation, random load change and sinusoidal load variation.

The system under consideration is a complex system with nonlinear components such as GDB, GRC, and the system parameters change randomly during operation. Types of loads are presented as shown in the Figure 10. At the same time, the system also considers other forms of renewable energy sources such as wind energy and solar energy.

- Step load disturbance : $\Delta P_{d1} = \Delta P_{d2} = 0.03\,(pu)$.
- Pulse load disturbance: $\Delta P_{d1} = \Delta P_{d2} = 0.03(pu)$, period: 40 second and pulse width: 10%.
- Random load disturbance with sample time is 40 seconds.
- Sinusoidal load disturbance: $\Delta P_{d1} = \Delta P_{d2} = 0.03\sin(0.0628t)$.

Table 4: The parameters used for simulation of two areas [25]

Area with non-reheat Turbin	Value	Area with Reheat Turbin	Value
M_1 (p.u.s)	10	M_2 (p.u.s)	10
D_1 (p.u./Hz)	1	D_2 (p.u./Hz)	1
T_{ch1} (s)	0.3	T_{ch2} (s)	0.3
T_{g1} (s)	0.1	T_{g2} (s)	0.2
R_1 (Hz/p.u.)	0.05	R_2 (Hz/p.u.)	0.05
B_1 (p.u./Hz)	21	B_2 (p.u./Hz)	21
T_1 (p.u./rad.)	22.6	T_2 (p.u./rad.)	22.6
T_{wts} (s)	1,5	F_{hp}	0.3
T_{spv} (s)	1,8	T_{rh}(s)	7

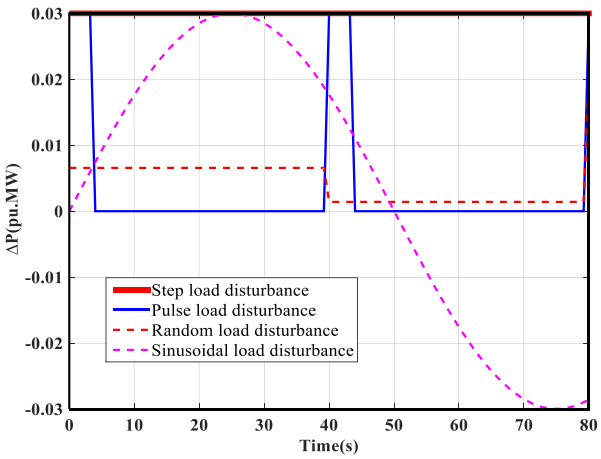

Figure 10: Types of load disturbances

Controller parameters for different load disturbances are presented in tables from Table 5 to Table 8 (with parameter of FPID controller is K_{p1}=0.67, K_{i1}=-0.4006, K_{d1}=-0.991, K_{p2}=-0.3266, K_{i2}=-0.2946, K_{d2}=-1 [25]).

Table 5: Parameters of controller in case step load disturbance

Type of Controllers	Parameters of controller			
	K_{p1}	K_{i1}	K_{p2}	K_{i2}
GA PI	-0.39	0.28	0.53	0.25
PSO PI	0.18	-0.25	-0.25	-0.25
GWO PI	0.10	-0.12	-0.12	-0.11
PSO GWO PI	0.43	-0.29	-0.5	-0.28
IGWO PI	0.42	-0.29	-0.54	-0.28

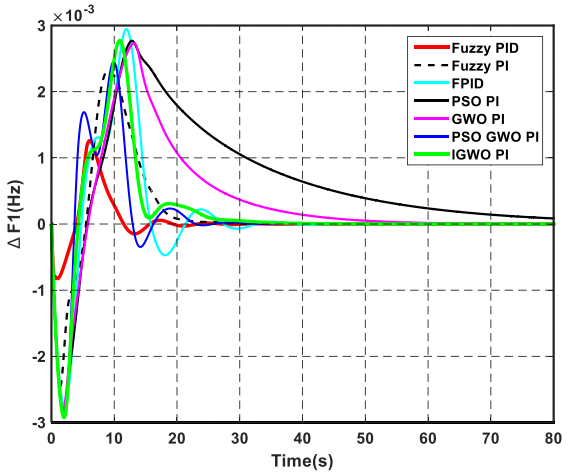

(a)

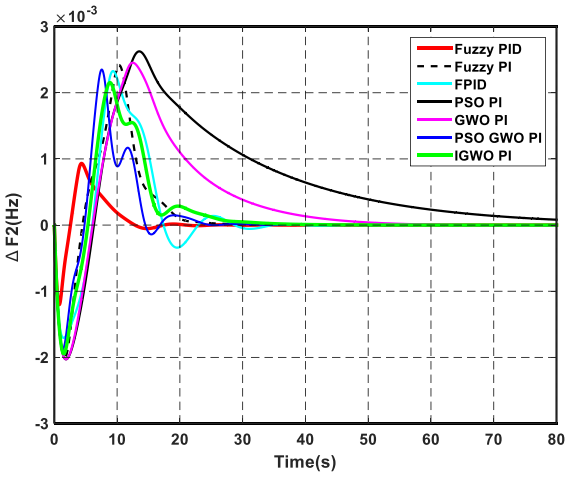

(b)

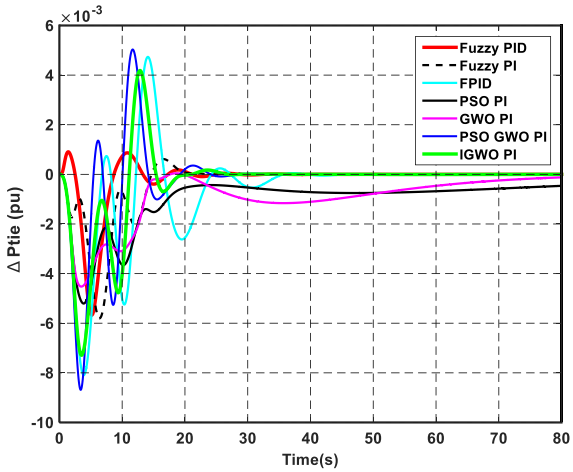

(c)

Figure 11: Dynamic responses to the step load disturbance in two areas

(a) ΔF1, (b) ΔF2, (c) ΔPtie

The performance of proposed fuzzy PID controller is compared with Genetic Algorithm tuned PI (GA PI), Grey Wolf Optimizer tuned PI (GWO PI), Particle Swarm Optimization optimized PI controller (PSO PI), Improved Grey Wolf Optimizer tuned PI (I- GWO PI), PSO GWO PI fuzzy PI controller and Fractional PID (FPID) to verify its control quality. Consequently, better system performance in terms of minimum settling times in frequency deviations is achieved with proposed fuzzy PID controller in comparison with other approaches . To study the dynamic performance of the proposed controllers, a step load disturbance in two areas and the system dynamic responses are shown in Figure 10. The simulation results with some published approaches such as with Genetic Algorithm tuned PI (GA PI), Grey Wolf Optimizer tuned PI (GWO PI), Particle Swarm Optimization optimized PI controller (PSO PI), Improved Grey Wolf Optimizer tuned PI (I- GWO PI), PSO GWO PI fuzzy PI controller and Fractional PID (FPID) to verify its control quality for the same power system are also shown in Figure 11. Critical analysis of the dynamic responses clearly reveals that significant improvement is observed with proposed fuzzy PID controller compared to other approaches reported in the literature.

Table 6: Parameters of controller in case pulse load disturbance

Type of Controllers	Parameters of controller			
	K_{p1}	K_{i1}	K_{p2}	K_{i2}
GA PI	0.05	-0.07	-0.58	0.11
PSO PI	0.1	0.1	-0.08	0.03
GWO PI	0.1	-0.12	-0.12	-0.11
PSO GWO PI	0.07	-0.02	-0.08	0.03
IGWO PI	0.04	-0.07	-0.58	0.11

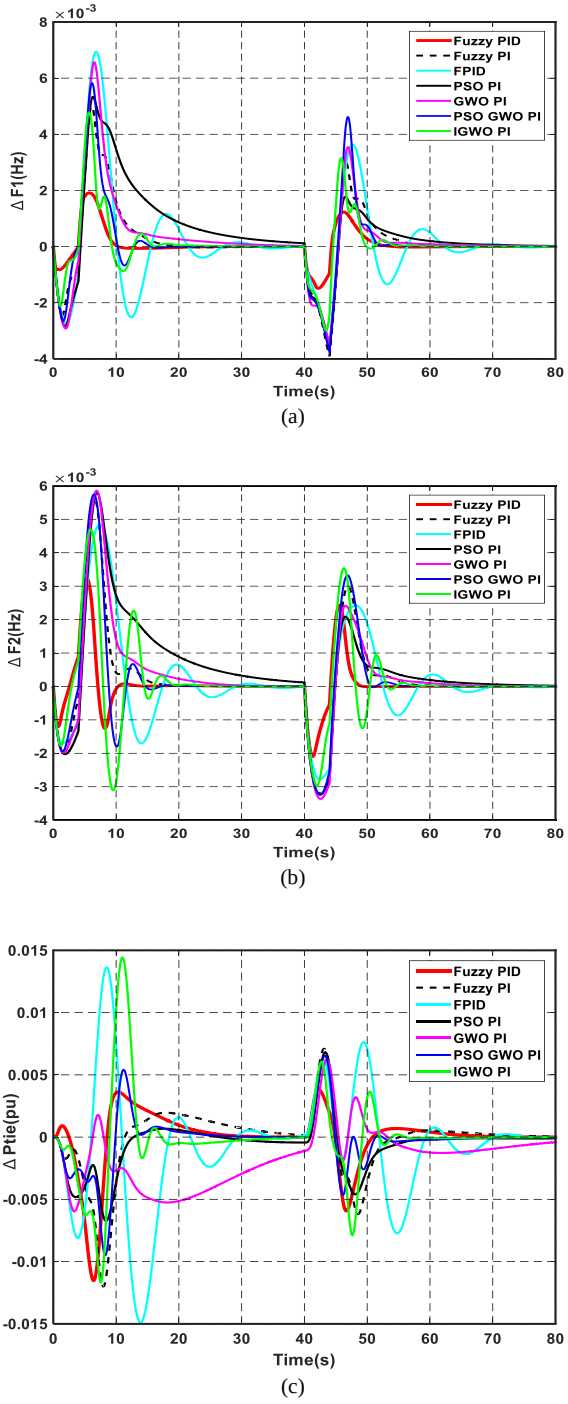

(a)

(b)

(c)

Figure 12: Dynamic responses to the pulse load disturbance in two areas

(a) ΔF1, (b) ΔF2, (c) ΔPtie

Table 7: Parameters of controller in case random load disturbance

Type of Controllers	Parameters of controller			
	K_{p1}	K_{i1}	K_{p2}	K_{i2}
GA PI	-0.95	-0.56	-1.34	-0.54
PSO PI	-0.45	-0.22	-0.5	-0.25
GWO PI	-0.03	-0.12	-0.12	-0.12
PSO GWO PI	0.15	-0.48	-0.5	-0.45
IGWO PI	-1.61	-1.69	-3.35	-1.72

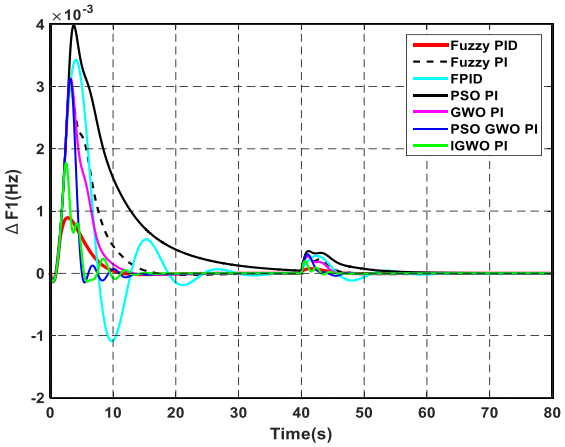

(a)

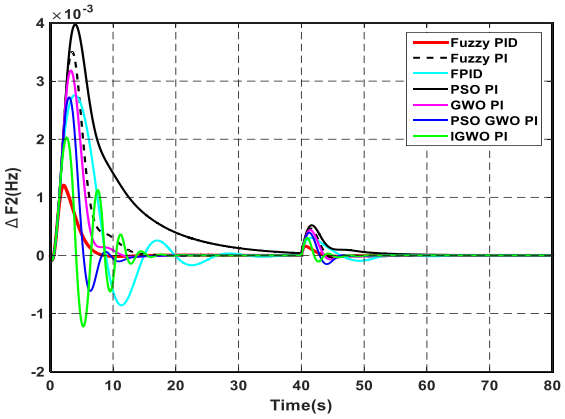

(b)

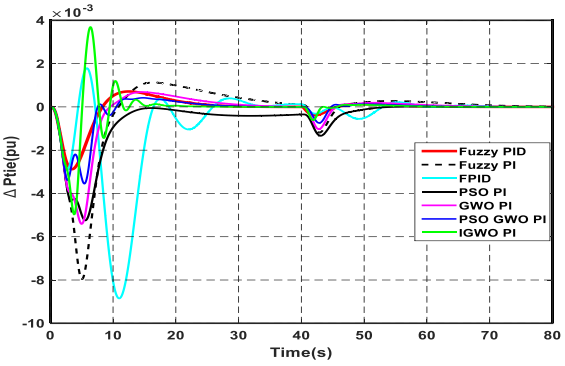

(c)

Figure 13: Dynamic responses to the random load disturbance in two areas (a) ΔF1, (b) ΔF2, (c) ΔPtie

Table 8: Parameters of controller in case sinusoidal Load disturbance

Type of Controllers	Parameters of controller			
	K_{p1}	K_{i1}	K_{p2}	K_{i2}
GA PI	-2.27	-1.57	-3.58	-1.72
PSO PI	-0.15	-0.59	-0.99	-0.61
GWO PI	-0.2	-0.2	-0.38	-0.5
PSO GWO PI	0.16	-0.47	-0.5	-0.5
IGWO PI	-2.16	-2.28	-4	-2.47

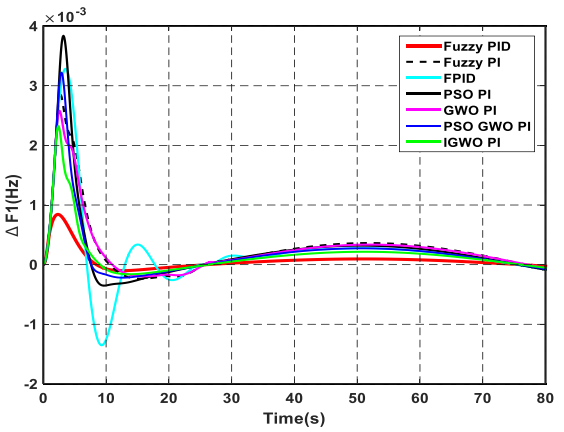

(a)

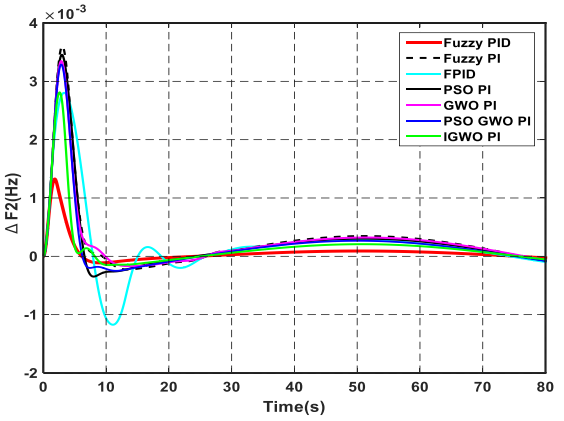

(b)

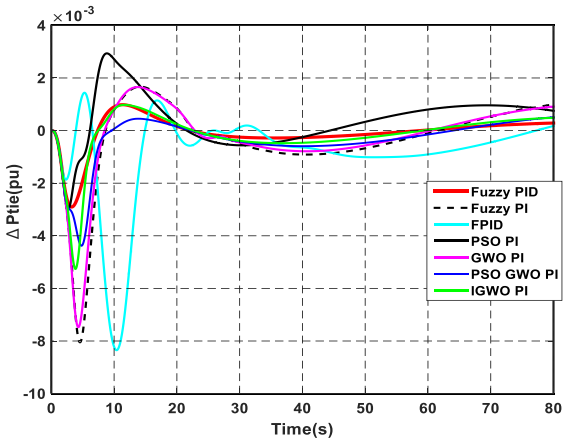

(c)

Figure 14: Dynamic responses to the sinusoidal load disturbance in two areas (a) ΔF1, (b) ΔF2, (c) ΔPtie

The simulation results shown in Figure 12-14 show that the frequency difference output response of the two regions has a stable time of about 7 to 10 seconds, very low overshoot and no frequency oscillations. when using fuzzy - PID controller. The above results have completely proved the optimality of the proposed controller. In this section, when the system exists load disturbances, these undesirable effects will be minimized under the initiative of the proposed controller.

4.2. Simulate the system when the system has nonlinear components such as: GDB (regulator deadband), GRC (generator speed limit) and uncertainty parameters

The fact is that nonlinear components such as GDB and GRC together with the uncertainty of the parameters are very suitable for practical control systems. A truly interconnected electrical system naturally includes such components. The nonlinearities, GDB and GRC, can be directly related to the operation of the power system. Meanwhile, the uncertainty related to the change of system parameters as illustrated in Table 8 clearly affects the stability of the power system. In this subsection, these undesirable effects will be mitigated under the positive capabilities of the proposed PID fuzzy logic controllers.

The simulation results when embedding the nonlinearities and uncertainties given in Table 8 are depicted in Figure 15. As can be seen, the negative influence of these variations has been successfully restrained. Both frequency and link power deviations are still eliminated with good control performance such as low overshoot and short stabilization time. These results fully demonstrate the robustness of the proposed fuzzy logic based load frequency controllers.

Table 9: Variations of the parameters

Tg1	0.1 ± 0.1*50%
Tg2	0.2 ± 0.1*50%
M1	10 ± 0.1*50%
D1	1 ± 1*50%
M2	10 ± 0.1*50%
D2	1 ± 1*50%
GRC	5%
GDB	5%

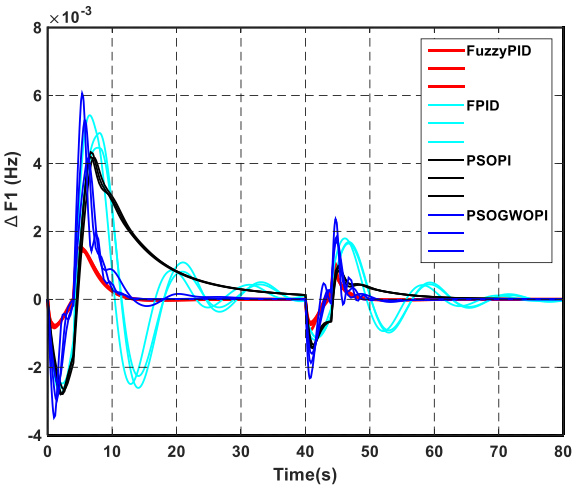

(a)

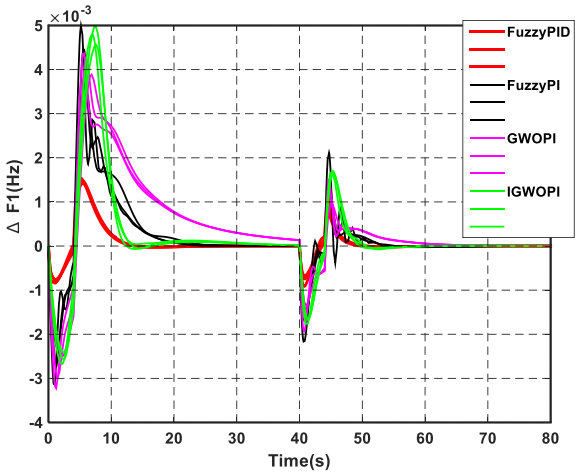

(b)

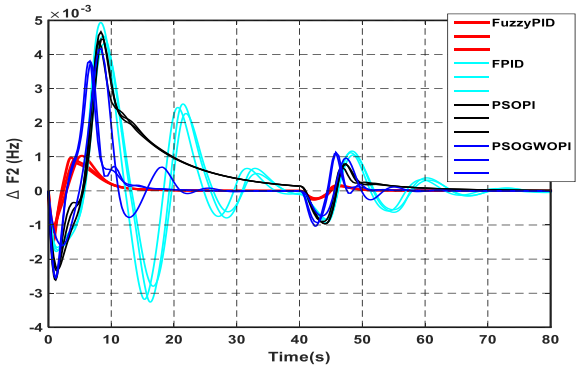

(c)

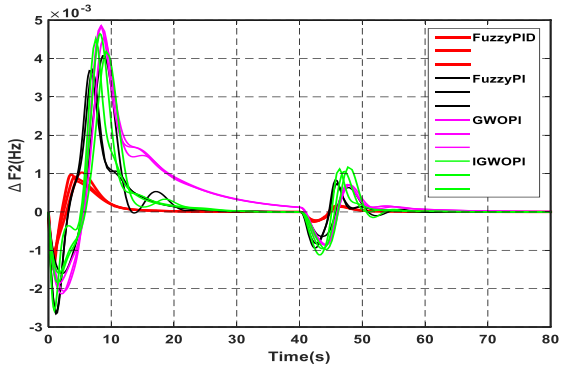

(d)

Figure 15: Dynamic responses to the step-load disturbance in two areas (with uncertainty parameters), (a) and (b): ΔF1, (c) and (d): ΔF2

5. Conclusion and future works

In this paper, a comparative evaluation has been performed to examine the effectiveness of the proposed PID - like fuzzy logic controller. In order to provide realistic results, the studied fuzzy - PID controllers have been validated on the two-area thermal power system in which the physical constraints of the GRC, GDB and renewable energy resources have also been taken into the consideration. The comparative dynamic performance evaluations have been carried out under the step, random, pulse, sinusoidal load and the types of renewable energy sources such as wind energy and solar energy. The results have confirmed that fuzzy - PID controller achieves much better dynamic performances such as the largest minimum damping ratio and the smallest overshoots and settling

times of the network frequency oscillations. It is also verified that the proposed fuzzy - PID controller outperforms the traditional PSO - based PI controller, GA - based PI controller, GWO - based PI controller, PSOGWO - based PI controller, IGWO - based PI controller, Fuzzy PI controller and the FPID controller in stabilizing the power system. Future work will focus on testifying the feasibility of the proposed control strategy in various scenarios of modern electric power grids, e.g. adding renewable energy sources to traditional interconnected power network as shown in this study.

References

[1]. Elgerd OI. Electric energy systems theory – an introduction. 2nded. Tata McGraw Hill; 2000.

[2]. Bevrani H. Robust power system frequency control. Springer; 2009.

[3]. Tan W, "Decentralized load frequency controller analysis and tuning for multi - area power systems," Energy Convers Manage 2011;52(5):2015–23.

[4]. K. Jagatheesan, B. Anand, Nilanjan Dey and Amira S. Ashour, "Artificial Intelligence in Performance Analysis of Load Frequency Control in Thermal-Wind-Hydro Power Systems" International Journal of Advanced Computer Science and Applications (IJACSA),6(7),2015. http://dx.doi.org/10.14569/IJACSA.2015.060727

[5]. Jesraj Tataji Dundi, Anand Gondesi, Rama Sudha Kasibhatla and A. Chandrasekhar, "Design of Robust Quasi Decentralized Type-2 Fuzzy Load Frequency Controller for Multi Area Power System" International Journal of Advanced Computer Science andApplications(IJACSA),13(11),2022. http://dx.doi.org/10.14569/IJACSA.2022.0131172

[6]. Rout UK, Sahu RK, Panda S, "Design and analysis of different ialevolution algorithm based automatic generation control for interconnected power system," Ain Shams Eng J ,2012

[7]. K. Soleimani and J. Mazloum, "Designing a GA-Based Robust Controller For Load Frequency Control (LFC),"Eng. Technol. Appl. Sci. Res., vol. 8, no. 2, pp. 2633–2639, Apr. 2018. https://doi.org/10.48084/etasr.1592

[8]. E. Pathan, A. Abu Bakar, S. A. Zulkifi, M. H. Khan, H. Arshad, and M. Asad, "A Robust Frequency Controller based on Linear Matrix Inequality for a Parallel Islanded Microgrid," Eng. Technol. Appl. Sci. Res., vol. 10, no. 5, pp. 6264–6269, Oct. 2020. https://doi.org/10.48084/etasr.3769

[9]. Yonghui Sun, Yingxuan Wang, Zhinong Wei, Guoqiang Sun, and Xiaopeng Wu ," Robust H1 Load Frequency Control of Multi-area Power System With Time Delay,"A Sliding Mode Control Approach. IEEE/CAA Journal Of Automatica Sinica, 5(2) : 610-617, 2018

[10]. Ali ES, Abd-Elazim SM, "Bacteria foraging optimization algorithm based load frequency controller for interconnected power system," Int J Electr Power Energy Syst, 2011

[11]. S. Guner, A. Ozdemir, "Turkish Power System: From Conventional Past to Smart Future," Innovative Smart Grid Technologies (ISGT Europe), 2nd IEEE PES International Conference and Exhibition, 2011.

[12]. J. Dudiak, M. Kolcun, "Integration of Renewable Energy Sources to the Power System," 14th Environment and Electrical Engineering (EEEIC) International Conference, 2014.

[13]. L.Wng, Y.Lin, S. Ke, "Stability Analysis of on Offshore Wind Farm Connected to Taiwan Power System Using DIGSILENT," IEEE, OCEANS, TAIPEI,2014

[14]. L. Ochoa, D. Wilson, "Angle Constraint Active Management of Distribution Networks with Wind Power," IEEE PES Innovative Smart Grid Technologies Conference Europe (ISGT Europe), 2010 .

[15]. A. M. Majeed, R. Vireck, F. Oechsle, M. Braun, S. Tenbohlen, "Effects of Distributed Generators from Renewable Energy on the Protection System in Distribution Networks," 46th International Universities' Power Engineering Conference, 2011.

[16]. R. Mosobi,T. Chichi, S. Gao, "Modeling and Power Quality Analysis of Integrated Renewable Energy System," IEEE Eighteenth National Power Systems Conference (NPSC),2014

[17]. Hossain, M.J. & Mahmud, Md. Apel, " Renewable Energy Integration Challenges and Solutions," 10.1007/978-981-4585-27-9,2013

[18]. Bevrani, Watanabe, Mitani, "Power System Monitoring and Control," John Wiley & Sons: Hoboken, NJ, USA, 2014.

[19]. Küfeo ˘glu, S, Lehtonen, M, "Macroeconomic assessment of voltage sags," Sustainability, 2016.

[20]. Arora, Krishan & Kumar, Ashok & Kamboj, Vikram & Prashar, Deepak & Shrestha, Bhanu & Joshi, Gyanendra Prasad, "Impact of Renewable Energy Sources into Multi Area Multi-Source Load Frequency Control of Interrelated Power System,"Mathematics. 9. 186. 10.3390/math9020186, 2021.

[21]. Chen, Chunyu & Zhang, Kaifeng & Yuan, Kun & Teng, Xianliang, "Tie-Line Bias Control Applicability to Load Frequency Control for Multi-Area Interconnected Power Systems of Complex Topology," Energies, vol.10 , pp.78, 2017.

[22]. Surbhi Pande, Roohi Kansal, "Load Frequency Control of Multi Area System using Integral Fuzzy Controller," International Journal of Scientific & Technology Research Volume 9, pp.59-64, June 2015.

[23]. Abdelmoumène Delassi, SalemArif, LakhdarMokrani, "Load frequency control problem in interconnected power systems using robust fractional PIλD controller," Ain Shams Engineering Journal, vol.9, no.1, pp.77-88, March 2018.

[24]. F. U. A. Ahammad and S. Mandal, "Robust load frequency control in multi-area power system: An LMI approach," 2016 IEEE First International Conference on Control, Measurement and Instrumentation (CMI), Kolkata, pp. 136-140, 2016

[25]. Taher, S. A., Fini, M. H., & Aliabadi, S. F, "Fractional order PID controller design for LFC in electric power systems using imperialist competitive algorithm,"Ain Shams Engineering Journal, 5(1), 121-135, 2014.